


Violation of the two-time Leggett-Garg inequalities for a coarse-grained quantum field

Masaki Tani ^{*}, Kosei Hatakeyama [†], Daisuke Miki [‡], and Yuki Yamasaki [§]
Department of Physics, Kyushu University, 744 Motoooka, Nishi-Ku, Fukuoka 819-0395, Japan

Kazuhiro Yamamoto ^{||}
Department of Physics, Kyushu University, 744 Motoooka, Nishi-Ku, Fukuoka 819-0395, Japan;
Research Center for Advanced Particle Physics, Kyushu University, 744 Motoooka, Nishi-ku, Fukuoka 819-0395, Japan;
and International Center for Quantum-field Measurement Systems for Studies of the Universe and Particles, KEK,
Oho 1-1, Tsukuba, Ibaraki 305-0801, Japan



(Received 6 November 2023; accepted 16 February 2024; published 15 March 2024)

We investigate the violation of the Leggett-Garg inequalities for a quantum field, focusing on the two-time quasiprobability distribution function of the dichotomic variable with a coarse-grained scalar field. The Leggett-Garg inequalities are violated depending on the quantum state of the field and the size of coarse graining. We demonstrate that the violation of the Leggett-Garg inequalities appears even for the vacuum state and the squeezed state by properly constructing the dichotomic variable and the projection operator.

DOI: [10.1103/PhysRevA.109.032213](https://doi.org/10.1103/PhysRevA.109.032213)

I. INTRODUCTION

The Leggett-Garg inequalities were proposed to test the macrorealism to characterize classical systems [1,2], in which a macroscopic system is in a definite state at any given time in different available states and the state can be measured without any effect on the system. However, this can be violated in quantum systems as a result of the superposition principle and the state collapse. The Leggett-Garg inequalities utilize temporal correlations [3], which are formulated in a similar way to the Clauser-Horne-Shimony-Holt inequality [4], to test the spatial nonlocal correlation and the violation of the realism. The violation of the Leggett-Garg inequalities has been experimentally verified in many macroscopic quantum systems, e.g., spin operators in qubit systems, superconducting circuits, and neutron interferometer [5–10]. The Leggett-Garg inequalities have also been applied to a test of the neutrino oscillations coherence [11] and single- and multiqubit systems on a quantum computer [12]. The quantum nature of gravitational interaction might be probed using the violation of the Leggett-Garg inequalities in the future [13].

Theoretical research on the Leggett-Garg inequalities is progressing (e.g., [14–16]). In the present paper we develop a theoretical formula for testing the violation of the Leggett-Garg inequalities in a quantum field theory. We utilize the two-time quasiprobability distribution function introduced in Ref. [17] and explored in Refs. [18–21]. The present work is a generalization of the theoretical work for a harmonic oscillator in Ref. [22], in which the violation of the two-time Leggett-Garg inequalities was investigated for various

quantum states and projection operators. (For studies of the violation of the Leggett-Garg inequalities in a harmonic oscillator, see also Refs. [23–26] and cf. Ref. [27].) In Ref. [22], a new technique to compute the two-time quasiprobability distribution function was developed. By generalizing the formulation to a quantum field, we demonstrate that the Leggett-Garg inequalities are violated for the dichotomic variable with a spatially coarse-grained quantum field, which will be useful to verify the quantum nature of a field.

The present paper is organized as follows. In Sec. II we briefly review the two-time quasiprobability distribution function and present the formulation for a quantum field theory in $(3 + 1)$ -dimensional Minkowski space-time. We demonstrate that the violation of the Leggett-Garg inequalities appears for a one-mode coherent state in the quantum field, and the conditions for the violation are clarified. We discuss the effect of the squeezing of the quantum state of the field on the violation of the Leggett-Garg inequalities. We also discuss a nontrivial extension of the dichotomic variable and the projection operator, which reveals the violation of the Leggett-Garg inequalities for the vacuum state and the squeezed state. In Sec. III we demonstrate a similar violation for a chiral massless field in $(1 + 1)$ -dimensional Minkowski space-time. Section IV is devoted to a summary and conclusions. In the Appendix, a brief summary of performing the integration of Eq. (30) is presented.

II. LEGGETT-GARG INEQUALITIES

We start with a brief review of the Leggett-Garg inequalities with the two-time quasiprobability distribution function. We introduce a dichotomic variable Q , which takes values ± 1 , and we assume that Q_1 and Q_2 are the values of Q by measurement at times t_1 and t_2 , respectively. Here s_1 and s_2 are the numbers ± 1 , which we choose for the measurements at t_1 and t_2 , respectively. Then we have $(1 + s_1 Q_1)(1 + s_2 Q_2) \geq 0$. Within the framework of macrorealism, there exists a joint

^{*}tani.masaki.898@s.kyushu-u.ac.jp

[†]hatakeyama.kosei.103@s.kyushu-u.ac.jp

[‡]miki.daisuke.454@s.kyushu-u.ac.jp

[§]yamasaki.yuuki.766@s.kyushu-u.ac.jp

^{||}yamamoto@phys.kyushu-u.ac.jp

probability function $p(Q_1, Q_2)$ to give the expectation values, which take the values of $0 \leq p(Q_1, Q_2) \leq 1$; then the expectation value of $(1 + s_1 Q_1)(1 + s_2 Q_2)$ must be non-negative:

$$(1 + s_1 Q_1)(1 + s_2 Q_2) \geq 0. \quad (1)$$

This is a simple explanation of the two-time Leggett-Garg inequalities. Thus, depending on the choice of s_1 and s_2 , we have four inequalities for the two times t_1 and t_2 . In the quantum theory, the corresponding two-time Leggett-Garg inequalities are expressed regarding $\hat{Q}(t)$ as a Heisenberg operator of a dichotomic quantum variable, which gives ± 1 by a measurement. Corresponding variables \hat{Q}_1 and \hat{Q}_2 are defined by the results of measurements of $\hat{Q}(t_1) = e^{i\hat{H}t_1} \hat{Q} e^{-i\hat{H}t_1}$ and $\hat{Q}(t_2) = e^{i\hat{H}t_2} \hat{Q} e^{-i\hat{H}t_2}$, respectively, where we assume that the system evolves unitarily through the Hamiltonian \hat{H} . The two-time quasiprobability function is introduced as

$$q_{s_1, s_2}(t_1, t_2) = \frac{1}{8} \text{Tr} \{ [1 + s_1 \hat{Q}(t_1)] [1 + s_2 \hat{Q}(t_2)] \rho_0 \} + (1 \leftrightarrow 2), \quad (2)$$

where ρ_0 is the initial density operator. Introducing the projection operator $\hat{P}_s = (1 + s\hat{Q})/2$ and its Heisenberg operator as

$$\hat{P}_s(t) = e^{i\hat{H}t} \hat{P}_s e^{-i\hat{H}t} = \frac{1}{2} e^{i\hat{H}t} (1 + s\hat{Q}) e^{-i\hat{H}t} = \frac{1}{2} [1 + s\hat{Q}(t)], \quad (3)$$

the quasiprobability distribution function is written as

$$q_{s_1, s_2}(t_1, t_2) = \frac{1}{2} \text{Tr} [\hat{P}_{s_1}(t_1) \hat{P}_{s_2}(t_2) \rho_0] + (1 \leftrightarrow 2) \\ = \text{Re Tr} [\hat{P}_{s_2}(t_2) \hat{P}_{s_1}(t_1) \rho_0]. \quad (4)$$

We note that $q_{s_1, s_2}(t_1, t_2)$ satisfies the relations of the probability [20]

$$\langle \hat{Q}(t_1) \rangle = \sum_{s_1, s_2 = \pm 1} s_1 q_{s_1, s_2}(t_1, t_2), \quad (5)$$

$$\langle \hat{Q}(t_2) \rangle = \sum_{s_1, s_2 = \pm 1} s_2 q_{s_1, s_2}(t_1, t_2), \quad (6)$$

$$\frac{1}{2} \langle \{ \hat{Q}(t_1), \hat{Q}(t_2) \} \rangle = \sum_{s_1, s_2 = \pm 1} s_1 s_2 q_{s_1, s_2}(t_1, t_2), \quad (7)$$

where $\{ \hat{Q}(t_1), \hat{Q}(t_2) \} = \hat{Q}(t_1) \hat{Q}(t_2) + \hat{Q}(t_2) \hat{Q}(t_1)$. However, $q_{s_1, s_2}(t_1, t_2)$ may have negative values in quantum theory; then we call $q_{s_1, s_2}(t_1, t_2)$ quasiprobability.

The above formula can be applied to a continuous quantum variable of a harmonic oscillator [21, 22, 24, 25]. In Ref. [22] a useful formula to compute the quasiprobability distribution function has been developed, which we apply to a quantum field in (3 + 1)-dimensional Minkowski space-time. In the present paper we consider a massless scalar field $\phi(x)$, expressed as

$$\hat{\phi}(t, \mathbf{x}) = \frac{1}{(2\pi)^{3/2}} \int d^3 k \\ \times \left(\frac{1}{\sqrt{2\omega_k}} e^{-i\omega_k t + i\mathbf{k} \cdot \mathbf{x}} \hat{a}_k + \frac{1}{\sqrt{2\omega_k}} e^{i\omega_k t - i\mathbf{k} \cdot \mathbf{x}} \hat{a}_k^\dagger \right), \quad (8)$$

where \hat{a}_k and \hat{a}_k^\dagger are the annihilation and creation operators satisfying $[\hat{a}_k, \hat{a}_{k'}^\dagger] = \delta^{(3)}(\mathbf{k} - \mathbf{k}')$, and $\omega_k = |\mathbf{k}|$. As the dichotomic operator, we adopt

$$Q(t) = \text{sgn}[\hat{\phi}(t) - \varphi(t)], \quad (9)$$

and the operator $\hat{\phi}(t)$ is defined by the coarse-grained field of $\hat{\phi}(x, t)$ using the Gaussian window function with the scale L as

$$\hat{\phi}(t) = \frac{1}{\pi^{3/2} L^3} \int d^3 x \hat{\phi}(x, t) e^{-x^2/L^2}, \quad (10)$$

where $\varphi(t)$ can be chosen arbitrarily. We note that $\hat{\phi}(x, t)$ should be understood as a Heisenberg operator. Then we may write $\hat{\phi}(t) = (2\pi)^{-3/2} \int d^3 k [u_k(t) \hat{a}_k + u_k^*(t) \hat{a}_k^\dagger]$, with $u_k(t) = e^{-i\omega_k t - k^2 L^2/4} / \sqrt{2\omega_k}$.

The projection operator is given by

$$P_s(t) = \frac{1}{2} [1 + s \text{sgn}[\hat{\phi}(t) - \varphi(t)]] = \theta(s[\hat{\phi}(t) - \varphi(t)]), \quad (11)$$

where $\theta(z)$ is the Heaviside function. The quasiprobability distribution function is

$$q_{s_1, s_2}(t_1, t_2) = \text{Re Tr} \{ \theta(s_2[\hat{\phi}(t_2) - \varphi(t_2)]) \theta(s_1[\hat{\phi}(t_1) - \varphi(t_1)]) \rho_0 \}. \quad (12)$$

The use of the mathematical formula $\theta'(z - c) = \delta(z - c) = (2\pi)^{-1} \int_{-\infty}^{\infty} dp e^{-ip(z-c)}$ allows us to write

$$\theta(s[\hat{\phi}(t) - \varphi(t)]) = \int_0^\infty dc \int_{-\infty}^\infty \frac{dp}{2\pi} e^{ip[-s(\hat{\phi}(t) - \varphi(t)) + c]}. \quad (13)$$

When the initial state ρ_0 at $t = 0$ is a pure state $\rho_0 = |\psi_0\rangle\langle\psi_0|$, we have

$$q_{s_1, s_2}(t_1, t_2) = \text{Re} \left[\int_0^\infty \int_0^\infty dc_1 dc_2 \int_{-\infty}^\infty \int_{-\infty}^\infty \frac{dp_1 dp_2}{(2\pi)^2} \right. \\ \times \langle \psi_0 | e^{-ip_2 s_2 \hat{\phi}(t_2)} e^{-ip_1 s_1 \hat{\phi}(t_1)} | \psi_0 \rangle e^{ip_2 [c_2 + s_2 \varphi(t_2)]} \\ \times e^{ip_1 [c_1 + s_1 \varphi(t_1)]} \left. \right]. \quad (14)$$

A. Coherent state

In this section we consider the initial state in which a mode ℓ is the coherent state and the other modes are the ground state, i.e., $|\psi_0\rangle = D_\ell(\xi) |0\rangle$, where $|0\rangle$ denotes the vacuum state. We define the displacement operator as

$$D_\ell(\xi) = \exp(\xi \hat{a}_\ell^\dagger - \xi^* \hat{a}_\ell) \quad (15)$$

and we have

$$D_\ell^\dagger(\xi) e^{-ip_2 s_2 \hat{\phi}(t_2)} e^{-ip_1 s_1 \hat{\phi}(t_1)} D_\ell(\xi) \\ = \exp(-\xi \hat{a}_\ell^\dagger + \xi^* \hat{a}_\ell) \\ \times \exp\left(-ip_2 s_2 \int \frac{d^3 k}{(2\pi)^{3/2}} [u_k(t_2) \hat{a}_k + u_k^*(t_2) \hat{a}_k^\dagger]\right) \\ \times \exp\left(-ip_1 s_1 \int \frac{d^3 k}{(2\pi)^{3/2}} [u_k(t_1) \hat{a}_k + u_k^*(t_1) \hat{a}_k^\dagger]\right) \\ \times \exp(\xi \hat{a}_\ell^\dagger - \xi^* \hat{a}_\ell). \quad (16)$$

Using the Baker-Campbell-Hausdorff formula $e^{X+Y} = e^X e^Y e^{-[X, Y]/2}$ and $e^X e^Y = e^{[X, Y]} e^X e^Y$, which hold for the operators X and Y satisfying $[X, Y] = \text{const}$, the quasiprobability

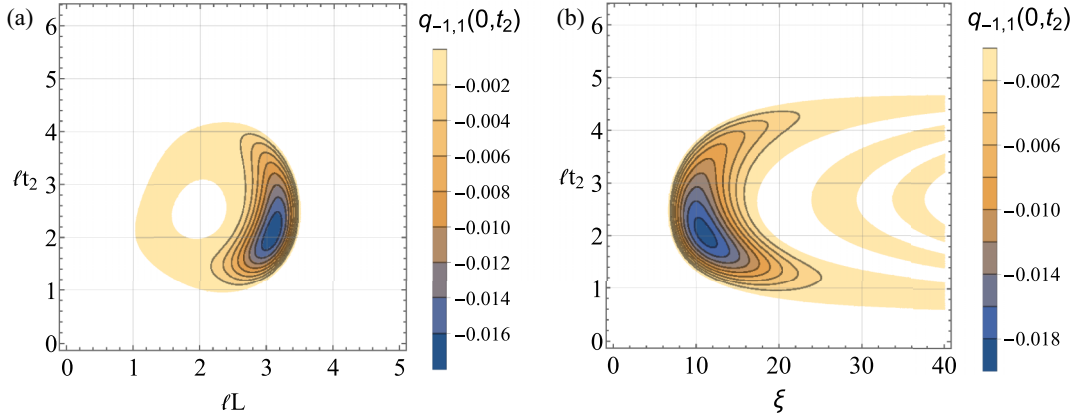


FIG. 1. (a) Contour of $q_{-1,1}(0, t_2)$ on the plane of ℓL and ℓt_2 , where we fixed $\xi = 8$. (b) Contour of $q_{-1,1}(0, t_2)$ on the plane of ξ and ℓt_2 , where we fixed $\ell L = 10/3$. In these panels, the quasiprobability takes negative values in the colored regions, where the Leggett-Garg inequality is violated.

function leads to

$$\begin{aligned}
 q_{s_1, s_2}(t_1, t_2) = & \text{Re} \left[\int_0^\infty \int_0^\infty dc_1 dc_2 \int_{-\infty}^\infty \int_{-\infty}^\infty \frac{dp_1 dp_2}{(2\pi)^2} \right. \\
 & \times \exp \left(-\frac{A}{2} (p_1^2 + p_2^2) - p_1 p_2 s_1 s_2 B \right. \\
 & \left. - i p_1 \{s_1 [E(t_1) - \varphi(t_1)] \right. \\
 & \left. \left. - c_1\} - i p_2 \{s_2 [E(t_2) - \varphi(t_2)] - c_2\} \right) \right], \quad (17)
 \end{aligned}$$

where A and B are defined by

$$A = \frac{1}{(2\pi)^3} \int d^3k \frac{1}{2\omega_k} e^{-L^2 k^2/2} = \frac{1}{4L^2 \pi^2}, \quad (18)$$

$$\begin{aligned}
 q_{s_1, s_2}(t_1, t_2) = & \text{Re} \left[\frac{1}{2\pi \sqrt{A^2 - B^2}} \int_0^\infty \int_0^\infty dc_1 dc_2 \exp \left(-\frac{1}{2(A^2 - B^2)} \{A(c_1^2 + c_2^2) - 2B s_1 s_2 c_1 c_2 \right. \right. \\
 & \left. \left. - 2s_1 [AE(t_1) - BE(t_2)] c_1 - 2s_2 [AE(t_2) - BE(t_1)] c_2 + A[E^2(t_1) + E^2(t_2)] - 2BE(t_1)E(t_2)\} \right) \right], \quad (21)
 \end{aligned}$$

which can be performed numerically, as demonstrated in Fig. 1. The appearance of the Leggett-Garg inequalities depends on the parameter of the amplitude of the coherent state ξ ($=\xi_\ell$) and on the size of the coarse graining L of the field through $E(t)$, A , and B . Figure 1 plots the contour of the quasiprobability distribution function $q_{-1,1}(0, t_2)$. Figure 1(a) plots $q_{-1,1}(0, t_2)$ on the plane of ℓL and ℓt_2 with fixed $\xi = 8$, where $\ell = |\ell|$. The colored regions are where the quasiprobability distribution function has negative values. Similarly, Fig. 1(b) shows $q_{-1,1}(0, t_2)$ on the plane of ξ and ℓt_2 , where ℓL is fixed as $\ell L = 10/3$. These figures demonstrate that the two-time Leggett-Garg inequality with $s_1 = -1$ and $s_2 = 1$ is violated when we choose the parameters ξ and L properly. The

$$\begin{aligned}
 B = & \frac{1}{(2\pi)^3} \int d^3k \frac{e^{-i\omega_k(t_2-t_1)}}{2\omega_k} e^{-L^2 k^2/2} \\
 = & \frac{1}{4L^2 \pi^2} - i \sqrt{\frac{\pi}{2}} \frac{e^{-(t_2-t_1)^2/2L^2}}{4L^3 \pi^2} (t_2-t_1) \left[1 - \text{erf} \left(\frac{i(t_2-t_1)}{\sqrt{2}L} \right) \right], \quad (19)
 \end{aligned}$$

with $\text{erf}(z)$ the error function, and $E(t)$ is defined by

$$E(t) = \frac{1}{(2\pi)^{3/2}} \sqrt{\frac{2}{\omega_\ell}} |\xi_\ell| e^{-L^2 t^2/4} \cos(\omega_\ell t - \alpha_\ell), \quad (20)$$

with $\xi_\ell = |\xi_\ell| e^{i\alpha_\ell}$. In the present paper we assume $\alpha_\ell = 0$. From Eq. (17) we note that the choice of the coherent state as the initial condition with $\varphi(t) = 0$ is equivalent to the choice of the vacuum state as the initial condition by choosing $\varphi(t) = -E(t)$. Therefore, we assume $\varphi(t) = 0$ in this section. By performing the Gaussian integral in Eq. (17), we have

results show that the optimized values are $\ell L \simeq \pi$ and $\xi \simeq 10$ for the violation. Thus the clear violation of the Leggett-Garg inequality occurs for the choice of $s_1 = -1$ and $s_2 = 1$. We found a violation for the case of $s_1 = -1$ and $s_2 = -1$, but the violation is very weak compared with the case of $s_1 = -1$ and $s_2 = 1$.

The behaviors of Fig. 1 can be understood as follows. We note that L is a parameter that represents the size of the coarse graining of the field. From Fig. 1(a), L must be taken to be $1 < \ell L < 3.5$ for the violation of the Leggett-Garg inequality. If L is much larger than the wavelength of the mode in the coherent state, $L\ell \gg 1$, the coherence in $\hat{\phi}(t)$ is washed out by the coarse graining of the field. Conversely, if L is much

shorter than the wavelength of the coherent state, $L\ell \ll 1$, the vacuum fluctuations of shorter-wavelength modes in $\hat{\phi}(t)$ have a measured value of $\hat{\phi}(t)$ that dominates the quantum nature of the mode ℓ in the coherent state. The optimized value is $\ell L \simeq \pi$, which means that L equals half of the wavelength of the coherent wave π/ℓ . From Fig. 1(b) we see that ξ , the magnitude of the coherent state parameter, must be greater than 7 for the violation. The optimized value is $\xi \simeq 10$, and then the violation of the Leggett-Garg inequalities gets weaker as ξ becomes larger.

The quasiprobability distribution function for a harmonic oscillator in a coherent state is periodic with respect to t_1 and t_2 with the period of the harmonic oscillator [22]. This is because the evolution of the system is unitary. In contrast, the quasiprobability distribution function for the coarse-grained quantum field shows no periodic behavior. The evolution of our system is unitary too, but this feature could be understood as an analog of the decoherence effect coming from the fact that the dichotomic variable for the field theory is constructed by the coarse graining of the field. This could be understood as a result of the quantum correlation in the field.

B. Squeezed state with a coherent mode

In this section we consider the initial state as the two-mode squeezed coherent state defined by

$$|\psi_0\rangle = D_\ell(\xi_\ell) \left(\prod_{\substack{k \\ (\text{independent})}} S_{k,-k}(\zeta_k) |0\rangle \right), \quad (22)$$

where $S_{k,-k}(\zeta_k)$ is the two-mode squeezed operator defined as $S_{k,-k}(\zeta_k) = \exp(\zeta_k^* a_k a_{-k} - \zeta_k a_k^\dagger a_{-k}^\dagger)$. We use the properties of the squeezing operator that transforms annihilation and creation operators as

$$S_{k,-k}^\dagger(\zeta_k) \hat{a}_k S_{k,-k}(\zeta_k) = \hat{a}_k \cosh r_k - \hat{a}_{-k}^\dagger e^{i\theta_k} \sinh r_k, \quad (23)$$

$$S_{k,-k}^\dagger(\zeta_k) \hat{a}_{-k}^\dagger S_{k,-k}(\zeta_k) = \hat{a}_{-k}^\dagger \cosh r_k - \hat{a}_k e^{-i\theta_k} \sinh r_k, \quad (24)$$

where we used $\zeta_k = r_k e^{i\theta_k}$. After a computation similar to that in the preceding section, we have the expression for the quasiprobability

$$q_{s_1, s_2}(t_1, t_2) = \text{Re} \int_0^\infty \int_0^\infty dc_1 dc_2 \int_{-\infty}^\infty \int_{-\infty}^\infty \frac{dp_1 dp_2}{(2\pi)^2} \exp \left[-\frac{A_{\text{sq}}(t_1)p_1^2 + A_{\text{sq}}(t_2)p_2^2}{2} - p_1 p_2 s_1 s_2 B_{\text{sq}}(t_1, t_2) - ip_1 \{s_1[E(t_1) - \varphi(t_1)] - c_1\} - ip_2 \{s_2[E(t_2) - \varphi(t_2)] - c_2\} \right], \quad (25)$$

where we defined

$$A_{\text{sq}}(t) = \frac{1}{(2\pi)^3} \int d^3k \frac{e^{-L^2 k^2/2}}{2\omega_k} [\cosh 2r_k - \sinh 2r_k \cos(2\omega_k t - \theta_k)], \quad (26)$$

$$B_{\text{sq}}(t_1, t_2) = \frac{1}{(2\pi)^3} \int d^3k \frac{e^{-L^2 k^2/2}}{2\omega_k} \{e^{-i\omega_k(t_2-t_1)} \cosh^2 r_k - \sinh 2r_k \cos[\omega_k(t_1+t_2) - \theta_k] + e^{i\omega_k(t_2-t_1)} \sinh^2 r_k\}, \quad (27)$$

and $E(t)$ is defined by Eq. (20). Here we note that assuming the squeezed state with a coherent mode as the initial condition with $\varphi(t) = 0$ is equivalent to assuming the squeezed state as the initial condition with $\varphi(t) = -E(t)$. We assume $\varphi(t) = 0$ hereafter in this section. The case of the coherence state is reproduced by choosing $r_k = 0$.

When r_k does not depend on the mode k and $\theta_k = 0$, i.e., $r_k = r$, $A_{\text{sq}}(t)$ and $B_{\text{sq}}(t_1, t_2)$ reduce to

$$A_{\text{sq}}(t) = \frac{Le^{-2r} - it\sqrt{2\pi}e^{-2t^2/L^2} \text{erf}(i\sqrt{2}t/L) \sinh 2r}{4\pi^2 L^3}, \quad (28)$$

$$B_{\text{sq}}(t_1, t_2) = \frac{1}{4\sqrt{2}\pi^2 L^3} \left\{ \sqrt{2}e^{-2r}L - i\sqrt{\pi}(t_2 - t_1)e^{-(t_2-t_1)^2/2L^2} \left[1 - \text{erf}\left(\frac{i(t_2-t_1)}{\sqrt{2}L}\right) \cosh 2r \right] + i\sqrt{\pi}(t_1 + t_2)e^{-(t_1+t_2)^2/2L^2} \text{erf}\left(\frac{i(t_1+t_2)}{\sqrt{2}L}\right) \sinh 2r \right\}. \quad (29)$$

After integration of the right-hand side of Eq. (25) over p_1 and p_2 , we have

$$q_{s_1, s_2}(t_1, t_2) = \text{Re} \left[\frac{1}{2\pi \sqrt{A_{\text{sq}}(t_1)A_{\text{sq}}(t_2) - B_{\text{sq}}(t_1, t_2)^2}} \int_0^\infty \int_0^\infty dc_1 dc_2 \exp \left(-\frac{1}{2[A_{\text{sq}}(t_1)A_{\text{sq}}(t_2) - B_{\text{sq}}(t_1, t_2)^2]} \times \{A_{\text{sq}}(t_2)c_1^2 + A_{\text{sq}}(t_1)c_2^2 - 2s_1 s_2 B_{\text{sq}}(t_1, t_2)c_1 c_2 - 2c_1 s_1 [A_{\text{sq}}(t_2)E(t_1) - B(t_1, t_2)E(t_2)] - 2c_2 s_2 [A_{\text{sq}}(t_1)E(t_2) - B_{\text{sq}}(t_1, t_2)E(t_1)] + A_{\text{sq}}(t_2)E(t_1)^2 + A_{\text{sq}}(t_1)E(t_2)^2 - 2B_{\text{sq}}(t_1, t_2)E(t_1)E(t_2)\} \right) \right]. \quad (30)$$

Figure 2 shows the same plots as in Fig. 1 but for the squeezed state with a coherent mode Eq. (30) with $r = 0.5$. Figure 2(a)

plots the contour of $q_{-1,1}(0, t_2)$ on the plane of ℓL and ℓt_2 with fixed $\xi = 8$, while Fig. 2(b) shows the contour on the

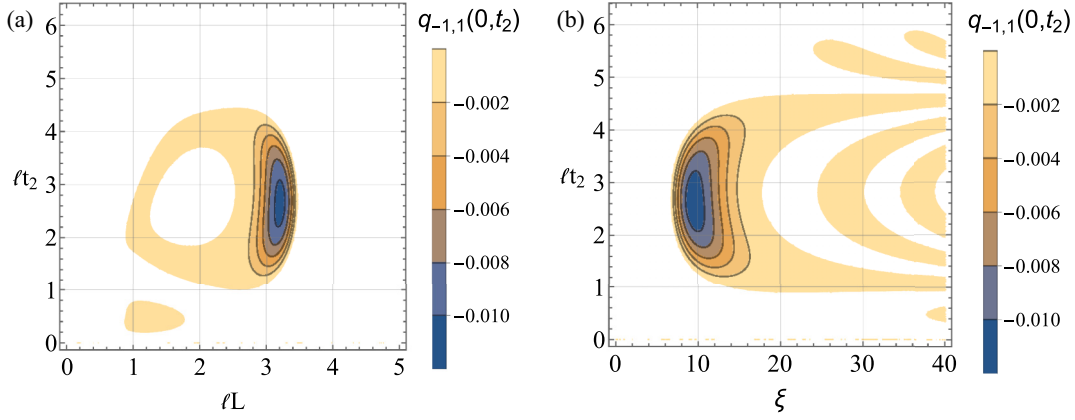


FIG. 2. Contour of $q_{-1,1}(0, t_2)$ for the squeezed state with a coherent mode. (a) Contour of $q_{-1,1}(0, t_2)$ on the plane of ℓL and ℓt_2 , where we fixed $\xi = 8$ and $r = 0.5$. (b) Contour of $q_{-1,1}(0, t_2)$ on the plane of ξ and ℓt_2 , where we fixed $\ell L = 10/3$ and $r = 0.5$.

plane of ξ and ℓt_2 with fixed $\ell L = 10/3$. The overall behavior of $q_{-1,1}(0, t_2)$ in Fig. 2 is similar to that of Fig. 1, though the effect of the squeezed initial state changes the pattern of the contour. The effect of squeezing increases the region where the Leggett-Garg inequality is violated. In particular, the periodic behavior appears in time t_2 when ξ is large, but it is not very clear because the violation is weak there.

C. Intuitive understanding of the violation

Let us discuss the reason why the violation of the Leggett-Garg inequalities appears. We investigated the Leggett-Garg inequalities in a quantum field theory, but it is useful to consider it in analogy with a harmonic oscillator [22]. The expectation value of the variable $\hat{\phi}(t)$ is given by

$$\begin{aligned} \text{Tr}[\hat{\phi}(t)\rho_0] &= \frac{1}{(2\pi)^{3/2}} \sqrt{\frac{2}{\omega_\ell}} |\xi_\ell| e^{-L^2 \ell^2/4} \cos(\omega_\ell t - \alpha_\ell) \\ &= E(t). \end{aligned} \quad (31)$$

As we have assumed $\alpha_\ell = 0$ in the present paper, the expectation value is $\text{Tr}[\hat{\phi}(t)\rho_0] = \bar{\phi}_0 \cos \omega_\ell t$, where $\bar{\phi}_0 = |\xi_\ell| e^{-L^2 \ell^2/4} / \sqrt{4\pi^3 \omega_\ell} > 0$. Figure 3 shows a schematic plot of the potential for $\bar{\phi}$ in analogy with a harmonic oscillator, which gives the solution $\bar{\phi}_0 \cos \omega_\ell t$. As we have also assumed $t_1 = 0$, the red mark in the figure denotes the

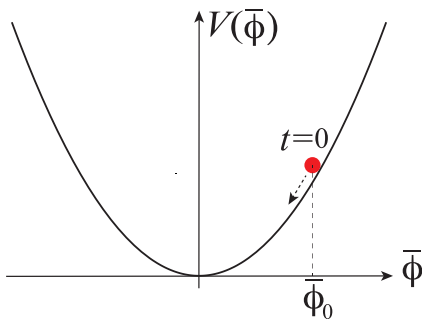


FIG. 3. Schematic plot of the potential $V(\bar{\phi})$ for $\bar{\phi}$. The violation of the Leggett-Garg inequality can be understood using an analogy of the dynamics of $\bar{\phi}$ as a harmonic oscillator.

initial position of $\bar{\phi}$ at $t_1 = 0$; then $\bar{\phi}$ starts to move to the left. As shown in the preceding section, the violation of the Leggett-Garg inequalities clearly occurs for $s_1 = -1$ and $s_2 = 1$. This means that the violation appears for the quasiprobability that the measurement at t_1 gives $\bar{\phi} < 0$ and the measurement at t_2 gives $\bar{\phi} > 0$. The results of these measurements are opposite to the expected values of $\text{Tr}[\hat{\phi}(t)\rho_0] = \bar{\phi}_0 \cos(\omega_\ell t)$. More specifically, the expectation values at t_1 and t_2 are $\text{Tr}[\hat{\phi}(t_1)\rho_0] > 0$ and $\text{Tr}[\hat{\phi}(t_2)\rho_0] < 0$ for $\pi/2 < \omega_\ell t_2 < 3\pi/2$. Because $\text{Tr}[\hat{\phi}(t)\rho_0] = \bar{\phi}_0 \cos(\omega_\ell t)$ can be regarded as a classically expected motion, the violation of the Leggett-Garg inequalities occurs when the measurements give values opposite to the classically expected values. This occurs in quantum mechanics because the wave function has a spread due to the superposition principle, which is the origin of the violation of realism.

D. Projection operator for the vacuum state and the squeezed state

In this section we adopt

$$Q(t) = 1 + \text{sgn}[\hat{\phi}(t) - w] + \text{sgn}[-\hat{\phi}(t) - w] \quad (32)$$

as a dichotomic operator, where the operator $\hat{\phi}(t)$ is defined by the coarse-grained field using the Gaussian window function with the scale L in a similar way to the preceding section. Here w is a parameter. The projection operator is given by

$$\begin{aligned} P_s(t) &= \frac{1}{2} \{1 + s + \text{sgn}[\hat{\phi}(t) - w] + \text{sgn}[-\hat{\phi}(t) - w]\} \\ &= \theta(s[\hat{\phi}(t) - w]) + \theta(-s[\hat{\phi}(t) + w]) + \frac{1}{2}(s - 1), \end{aligned} \quad (33)$$

where $\theta(z)$ is the Heaviside function. This dichotomic variable defined by the above projection operator is understood as follows. When the absolute value of a result of a measurement of the coarse-grained field $\hat{\phi}(t)$ is larger than w , we assign $Q = 1$. On the other hand, when the absolute value of a result of a measurement of $\hat{\phi}(t)$ is smaller than w , we assign $Q = -1$. Therefore, the projection operator P_s with $s = 1$ gives the projection onto the region $|\bar{\phi}(t)| > w$, while P_s with $s = -1$ gives the projection onto the region $|\bar{\phi}(t)| \leq w$.

The quasiprobability function is given by evaluating

$$q_{s_1, s_2}(t_1, t_2) = \text{Re Tr} \left[\left\{ \theta(s_2[\hat{\phi}(t_2) - w]) + \theta(-s_2[\hat{\phi}(t_2) + w]) + \frac{1}{2}(s_2 - 1) \right\} \right. \\ \left. \times \left\{ \theta(s_1[\hat{\phi}(t_1) - w]) + \theta(-s_1[\hat{\phi}(t_1) + w]) + \frac{1}{2}(s_1 - 1) \right\} \rho_0 \right]. \quad (34)$$

Using the mathematical formula $\theta'(z - a) = \delta(z - a) = \frac{1}{2\pi} \int_{-\infty}^{\infty} dp e^{-ip(z-a)}$, we have

$$q_{s_1, s_2}(t_1, t_2) = \text{Re} \left[\langle \psi_0 | \left(\int_0^{\infty} dc_2 \int_{-\infty}^{\infty} \frac{dp_2}{2\pi} (e^{-ip_2\{s_2[\hat{\phi}(t_2) - w] - c_2\}} + e^{ip_2\{s_2[\hat{\phi}(t_2) + w] + c_2\}}) + \frac{1}{2}(s_2 - 1) \right) \right. \\ \left. \times \left(\int_0^{\infty} dc_1 \int_{-\infty}^{\infty} \frac{dp_1}{2\pi} (e^{-ip_1\{s_1[\hat{\phi}(t_1) - w] - c_1\}} + e^{ip_1\{s_1[\hat{\phi}(t_1) + w] + c_1\}}) + \frac{1}{2}(s_1 - 1) \right) | \psi_0 \rangle \right], \quad (35)$$

where we assumed that the initial state ρ_0 at $t = 0$ is the squeezed state $\rho_0 = |\psi_0\rangle\langle\psi_0|$ with

$$|\psi_0\rangle = \left(\prod_{\substack{k \\ (\text{independent})}} S_{k, -k}(\zeta_k) \right) |0\rangle. \quad (36)$$

After calculations similar to those in the preceding section, we have the quasiprobability distribution function

$$q_{s_1, s_2}(t_1, t_2) = \text{Re} \left[2 \int_0^{\infty} \int_0^{\infty} dc_1 dc_2 \int_{-\infty}^{\infty} \int_{-\infty}^{\infty} \frac{dp_1 dp_2}{(2\pi)^2} \right. \\ \times \exp \left(-\frac{A_{\text{sq}}(t_1)p_1^2 + A_{\text{sq}}(t_2)p_2^2}{2} - p_1 p_2 s_1 s_2 B_{\text{sq}}(t_1, t_2) + ip_1(s_1 w + c_1) + ip_2(s_2 w + c_2) \right) \\ + 2 \int_0^{\infty} \int_0^{\infty} dc_1 dc_2 \int_{-\infty}^{\infty} \int_{-\infty}^{\infty} \frac{dp_1 dp_2}{(2\pi)^2} \\ \times \exp \left(-\frac{A_{\text{sq}}(t_1)p_1^2 + A_{\text{sq}}(t_2)p_2^2}{2} + p_1 p_2 s_1 s_2 B_{\text{sq}}(t_1, t_2) + ip_1(s_1 w + c_1) + ip_2(s_2 w + c_2) \right) \\ + 2 \int_0^{\infty} dc_1 \int_{-\infty}^{\infty} \frac{dp_1}{2\pi} \exp -\frac{A_{\text{sq}}(t_1)p_1^2}{2} + ip_1(s_1 w + c_1) \frac{1}{2}(s_2 - 1) \\ + 2 \int_0^{\infty} dc_2 \int_{-\infty}^{\infty} \frac{dp_2}{2\pi} \exp -\frac{A_{\text{sq}}(t_2)p_2^2}{2} + ip_2(s_2 w + c_2) \frac{1}{2}(s_1 - 1) + \frac{1}{4}(s_1 - 1)(s_2 - 1) \left. \right], \quad (37)$$

where $A_{\text{sq}}(t)$ and $B_{\text{sq}}(t_1, t_2)$ are defined by Eqs. (26) and (27), respectively. Here we assume that r_k does not depend on k and $\theta_k = \theta_0 = 0$, i.e., $r_k = r$. Equation (37) can be evaluated in a similar way to the preceding section,

$$q_{s_1, s_2}(t_1, t_2) = \text{Re} \left\{ \frac{1}{\pi \sqrt{A_{\text{sq}}(t_1)A_{\text{sq}}(t_2) - B_{\text{sq}}(t_1, t_2)^2}} \int_0^{\infty} \int_0^{\infty} dc_1 dc_2 \exp \left(-\frac{1}{2[A_{\text{sq}}(t_1)A_{\text{sq}}(t_2) - B_{\text{sq}}(t_1, t_2)^2]} \right. \right. \\ \times \{ A_{\text{sq}}(t_2)c_1^2 + A_{\text{sq}}(t_1)c_2^2 - 2s_1 s_2 B_{\text{sq}}(t_1, t_2)c_1 c_2 + 2c_1 s_1 w [A_{\text{sq}}(t_2) - B(t_1, t_2)] \\ + 2c_2 s_2 w [A_{\text{sq}}(t_1) - B_{\text{sq}}(t_1, t_2)] + [A_{\text{sq}}(t_2) + A_{\text{sq}}(t_1) - 2B_{\text{sq}}(t_1, t_2)] w^2 \} \\ \left. \left. + \frac{1}{\pi \sqrt{A_{\text{sq}}(t_1)A_{\text{sq}}(t_2) - B_{\text{sq}}(t_1, t_2)^2}} \int_0^{\infty} \int_0^{\infty} dc_1 dc_2 \exp \left(-\frac{1}{2[A_{\text{sq}}(t_1)A_{\text{sq}}(t_2) - B_{\text{sq}}(t_1, t_2)^2]} \right. \right. \right. \\ \times \{ A_{\text{sq}}(t_2)c_1^2 + A_{\text{sq}}(t_1)c_2^2 + 2s_1 s_2 B_{\text{sq}}(t_1, t_2)c_1 c_2 + 2c_1 s_1 w [A_{\text{sq}}(t_2) + B(t_1, t_2)] \\ + 2c_2 s_2 w [A_{\text{sq}}(t_1) + B_{\text{sq}}(t_1, t_2)] + [A_{\text{sq}}(t_2) + A_{\text{sq}}(t_1) + 2B_{\text{sq}}(t_1, t_2)] w^2 \} \\ \left. \left. + \frac{1}{2}(s_2 - 1) \left[1 - \text{erf} \left(\frac{s_1 w}{\sqrt{2A_{\text{sq}}(t_1)}} \right) \right] + \frac{1}{2}(s_1 - 1) \left[1 - \text{erf} \left(\frac{s_2 w}{\sqrt{2A_{\text{sq}}(t_2)}} \right) \right] + \frac{1}{4}(s_1 - 1)(s_2 - 1) \right\}. \quad (38)$$

Figure 4 plots the contour of $q_{1,1}(0, t_2)$ on the plane of wL and t_2/L , where $r = 0.3$ [Fig. 4(a)] and $r = 0.5$ [Fig. 4(b)].

We can see that the quasiprobability distribution function has negative values smaller than -0.03 and -0.025 for $r = 0.3$

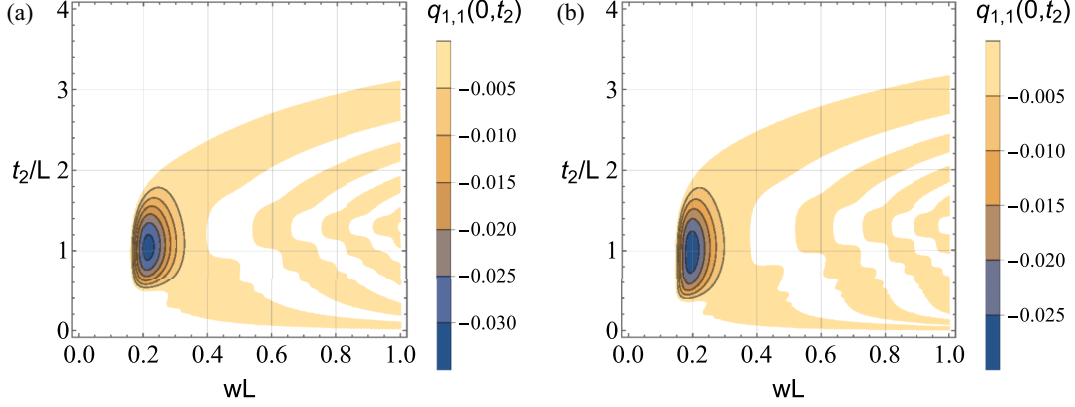


FIG. 4. Contour of $q_{1,1}(0, t_2)$ for the squeezed state with Eq. (33) on the plane of wL and t_2/L , where we fixed $\theta_0 = 0$ and (a) $r = 0.3$ and (b) $r = 0.5$. In these panels, the quasiprobability has negative values in the colored regions, where the Leggett-Garg inequality is violated.

and 0.5 [in Figs. 4(a) and 4(b), respectively] at $Lw \simeq 0.2$. Figure 5 plots the same contour as in Fig. 4 but for the case $r = 0$, the vacuum state. For the vacuum state and the squeezed states, the expectation values of $\hat{\phi}(t)$ are always zero. On the other hand, $q_{1,1}(0, t_2)$ denotes the quasiprobability that the measurement at $t_1 = 0$ gives $|\hat{\phi}(t_1)| > w$ and the measurement at t_2 gives $|\hat{\phi}(t_2)| > w$. This is the counterintuitive result of measurements against the expectation values. This occurs because of a spread of the wave function, coming from the superposition principle of the quantum-mechanical systems.

III. ONE-DIMENSIONAL CHIRAL MASSLESS SCALAR FIELD

In this section we consider a chiral massless quantum field in $(1 + 1)$ -dimensional Minkowski space-time motivated by Ref. [28]. We consider a massless scalar field, which is expressed as

$$\hat{\phi}(t, x) = \frac{1}{(2\pi)^{1/2}} \int_0^\infty dk \left(\frac{1}{\sqrt{2k}} e^{-i\omega_k(t+x)} \hat{a}_k + \frac{1}{\sqrt{2k}} e^{i\omega_k(t+x)} \hat{a}_k^\dagger \right), \quad (39)$$

where \hat{a}_k and \hat{a}_k^\dagger are the annihilation and creation operators satisfying $[\hat{a}_k, \hat{a}_{k'}^\dagger] = \delta(k - k')$, respectively, and $\omega_k = k$. As

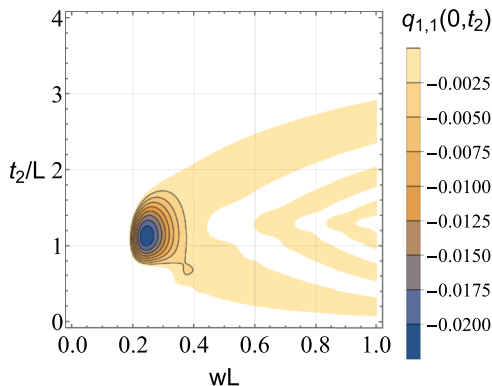


FIG. 5. Same as in Fig. 4 but for the case $r = 0$ and $\theta_0 = 0$, the vacuum state.

the dichotomic operator, we adopt

$$Q(t) = \text{sgn}[\hat{\phi}'(t) - \varphi(t)], \quad (40)$$

where we defined the operators $\hat{\phi}'(t)$ by the coarse-grained quantity of $\hat{\phi}'(x, t)$ using the Gaussian window function with the scale L as

$$\hat{\phi}'(t) = \frac{1}{\sqrt{\pi}L} \int_{-\infty}^{\infty} dx \hat{\phi}'(x, t) e^{-x^2/L^2}, \quad (41)$$

with $\phi'(t, x) = \partial\phi(x, t)/\partial x$, and $\varphi(t)$ can be chosen arbitrarily. Then we may have

$$\hat{\phi}'(t) = \frac{1}{\sqrt{2\pi}} \int_0^\infty dk [u_k(t) \hat{a}_k + u_k^*(t) \hat{a}_k^\dagger], \quad (42)$$

with $u_k(t) = ik e^{-ikt - k^2 L^2/4} / \sqrt{2k}$. The projection operator and the quasiprobability distribution function are given by

$$P_s(t) = \frac{1}{2} \{1 + s \text{sgn}[\hat{\phi}'(t) - \varphi(t)]\} = \theta[s[\hat{\phi}'(t) - \varphi(t)]], \quad (43)$$

$$q_{s_1, s_2}(t_1, t_2) = \text{Re Tr} \{ \theta[s_2[\hat{\phi}'(t_2) - \varphi(t_2)]] \theta[s_1[\hat{\phi}'(t_1) - \varphi(t_1)]] \rho_0 \}. \quad (44)$$

A. Coherent state

We first consider the initial state in which a mode ℓ is in the coherent state and the other modes are in the vacuum state, i.e., $|\psi_0\rangle = D_\ell(\xi)|0\rangle$. In this case, we have the same expression for the quasiprobability distribution function as Eq. (21) but with A , B , and $E(t)$ replaced by

$$\begin{aligned} A &= \frac{1}{2\pi} \int_0^\infty e^{-L^2 k^2/2} \frac{k^2}{2k} dk = \frac{1}{4\pi L^2}, \\ B &= \frac{1}{2\pi} \int_0^\infty e^{-L^2 k^2/2} \frac{e^{-ik(t_1 - t_2)}}{2k} k^2 dk \\ &= \frac{1}{4\pi L^2} - \frac{i}{4\pi L^3} e^{-(t_2 - t_1)^2/2L^2} (t_2 - t_1) \sqrt{\frac{\pi}{2}} \\ &\quad \times \left[1 - \text{erf} \left(\frac{i(t_2 - t_1)}{\sqrt{2}L} \right) \right], \end{aligned} \quad (45)$$

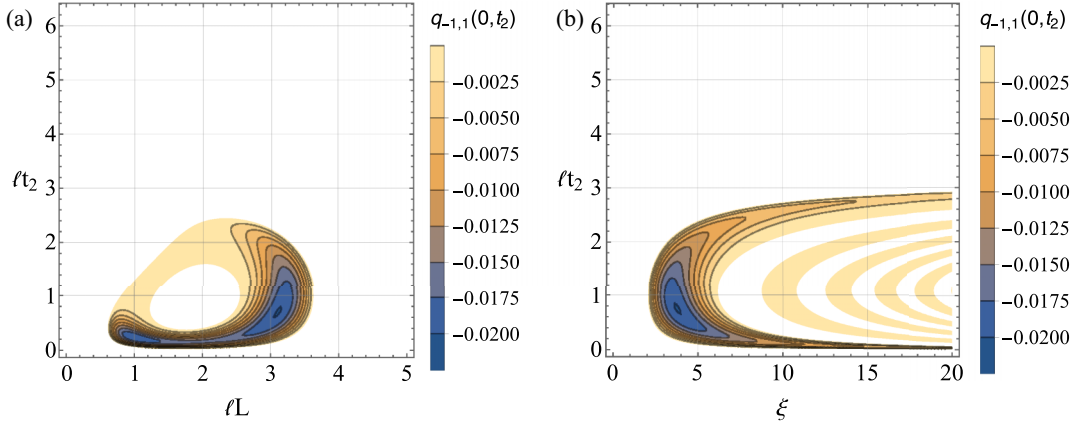


FIG. 6. Contour of $q_{-1,1}(0, t_2)$ for the one-mode coherent state of the field (a) on the plane of ℓL and ℓt_2 , where we fixed $\xi = 3$, and (b) on the plane of ξ and ℓt_2 , where we fixed $\ell L = 10/3$. In these panels, the quasiprobability takes negative values in the colored regions, where the Leggett-Garg inequality is violated.

and

$$E(t) = \sqrt{\frac{\omega_\ell}{\pi}} |\xi_\ell| e^{-L^2 \ell^2 / 4} \sin(\alpha_\ell - \omega_\ell t), \quad (47)$$

with $\xi = |\xi_\ell| e^{i\alpha_\ell}$. We assume $\alpha_\ell = 0$ in the present paper.

The quasiprobability distribution function can be evaluated numerically, as demonstrated in Fig. 6, which plots the contour of the quasiprobability distribution function $q_{-1,1}(0, t_2)$ on the plane of ℓL and ℓt_2 [Fig. 6(a)] and on the plane of ξ and ℓt_2 [Fig. 6(b)]. Behaviors similar to those in Fig. 1 can be seen. The appearance of the Leggett-Garg inequalities depends on the parameters of the amplitude of the coherent state ξ and on the size of the coarse graining L of the field through $E(t)$, A , and B . Figure 6(a) plots the contour on the plane of ℓL and ℓt_2 with fixed $\xi = 3$. The colored regions are where the quasiprobability distribution function has negative values. Similarly, Fig. 6(b) shows the contour on the plane of

ξ and ℓt_2 , where ℓL is fixed as $\ell L = 10/3$. The clear violation of the two-time Leggett-Garg inequalities appears for $s_1 = -1$ and $s_2 = 1$ when we choose the parameters ξ and L properly. The results show that the optimized values are $\ell L \simeq \pi$ and $\xi \simeq 4$.

B. Squeezed state with a coherent mode

We next consider the squeezed state with a coherent mode defined by $|\psi_0\rangle = D_\ell(\xi_\ell) [\prod_{k>0} S_k(\zeta_k)] |0\rangle$, where $S_k(\zeta_k)$ is the one-mode squeezing operator defined as

$$S_k(\zeta_k) = \exp\left(\frac{\zeta_k^* \hat{a}_k^2 - \zeta_k \hat{a}_k^{\dagger 2}}{2}\right). \quad (48)$$

In this case, we have the same expression for the quasiprobability distribution function as Eq. (25) but with $A_{\text{sq}}(t)$ and $B_{\text{sq}}(t_1, t_2)$ replaced by

$$A_{\text{sq}}(t) = \frac{1}{2\pi} \int_0^\infty dk e^{-L^2 k^2 / 2} \frac{k^2}{2k} [\cosh 2r_k - \sinh 2r_k \cos(2kt - \theta_k)], \quad (49)$$

$$B_{\text{sq}}(t_1, t_2) = \frac{1}{2\pi} \int_0^\infty dk e^{-L^2 k^2 / 2} \frac{k^2}{2k} \{ \cosh 2r_k \cos[k(t_1 - t_2)] - \sinh 2r_k \cos[k(t_1 + t_2) - \theta_k] + i \sin[k(t_1 - t_2)] \}, \quad (50)$$

and $E(t)$ defined by Eq. (47), where $\zeta_k = r_k e^{i\theta_k}$. Equations (49) and (50) yield

$$A_{\text{sq}}(t) = \frac{L(\cosh 2r - \cos \theta \sinh 2r) + e^{-2r^2/L^2} \sqrt{2\pi} t [-i \cos \theta \operatorname{erf}(i\sqrt{2}t/L) - \sin \theta] \sinh 2r}{4\pi L^3}, \quad (51)$$

$$B_{\text{sq}}(t_1, t_2) = \frac{1}{4\sqrt{2}L^3\pi} \left(-i\sqrt{\pi}(t_2 - t_1) + \cosh 2r \left[\sqrt{2}L - e^{-(t_2-t_1)^2/2L^2} \sqrt{\pi}(t_2 - t_1) \operatorname{erf}\left(-\frac{i(t_2 - t_1)}{\sqrt{2}L}\right) \right] - \sinh 2r \left\{ \sqrt{2}L \cos \theta + i e^{-(t_2+t_1)^2/2L^2} \sqrt{\pi}(t_2 + t_1) \left[\cos \theta \operatorname{erf}\left(\frac{i(t_2 + t_1)}{\sqrt{2}L}\right) - i \sin \theta \right] \right\} \right) \quad (52)$$

when ζ_k does not depend on k , i.e., $\zeta_k = r$ and $\theta_k = \theta$. In this case, we have the same expression for the quasiprobability distribution function as Eq. (30) but with $A_{\text{sq}}(t)$, $B_{\text{sq}}(t_1, t_2)$, and $E(t)$ defined by Eqs. (51), (52), and (47), respectively.

Figure 7 shows the contour of the quasiprobability distribution function $q_{-1,1}(0, t_2)$. Figure 7(a) plots the contour of $q_{-1,1}(0, t_2)$ on the plane of ℓL and ℓt_2 with fixed $\xi = 3$; Fig. 7(b) shows the contour on the plane of ξ and ℓt_2 with fixed $\ell L = 10/3$. In Fig. 7 we assumed $r_k = 0.5$ and $\theta_k = 0$.

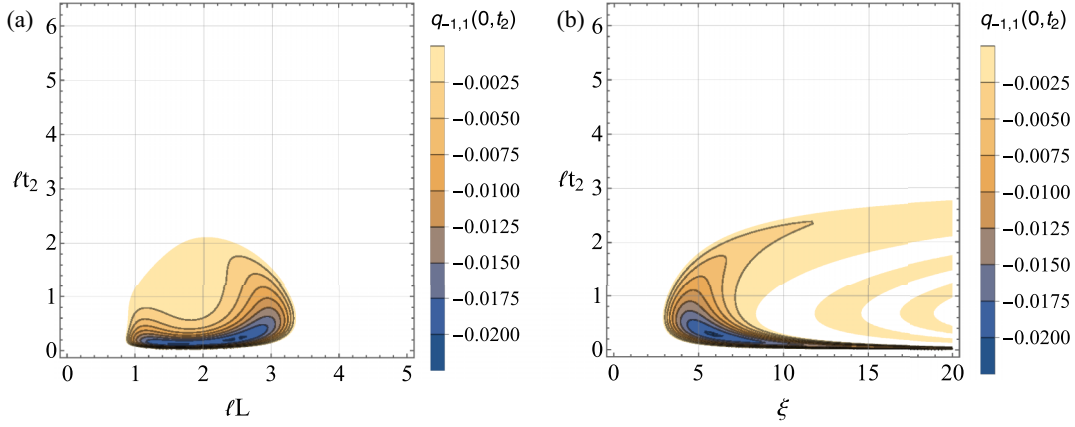


FIG. 7. Same as Fig. 6 but for the squeezed field with a coherent mode with $r_k = r = 0.5$ and $\theta_k = 0$. (a) Contour of $q_{-1,1}(0, t_2)$ on the plane of lL and $l t_2$, where we fixed $\xi = 3$. (b) Contour of $q_{-1,1}(0, t_2)$ on the plane of ξ and $l t_2$, where we fixed $lL = 10/3$.

Similarly to Fig. 6, $q_{-1,1}(0, t_2)$ in Fig. 7 has negative values in the colored region in each panel. The overall behavior of $q_{-1,1}(0, t_2)$ in Fig. 7 is similar to that of Fig. 6, though the effect of the squeezed initial state changes the pattern of the contour.

We can understand when the violation of the Leggett-Garg inequalities appears in a way to similar the three-dimensional case. For the one-dimensional chiral field, the expectation value of the coarse-grained field is

$$\text{Tr}[\hat{\phi}'(t)\rho_0] = \sqrt{\frac{\omega_\ell}{\pi}} |\xi_\ell| e^{-L^2 \ell^2/4} \sin(\alpha_\ell - \omega_\ell t) = E(t). \quad (53)$$

As we assumed $\alpha_\ell = 0$, $\text{Tr}[\hat{\phi}'(t)\rho_0]$ takes negative values for $0 < \omega_\ell t < \pi$. On the other hand, $q_{-1,1}(0, t_2)$ is the quasiprobability that the measurement of $\hat{\phi}'(t)$ at t_2 gives a positive value, which is opposite to the expectation values for $0 < \omega_\ell t < \pi$, where the violation of the Leggett-Garg inequality appears as demonstrated in Figs. 6 and 7.

C. Projection operator for the squeezed state and the vacuum state

Similarly to Sec. II C, let us now consider the case when the dichotomic variable $Q(t)$ is adopted as

$$Q(t) = 1 + \text{sgn}[\hat{\phi}'(t) - w] + \text{sgn}[-\hat{\phi}'(t) - w], \quad (54)$$

in which the projection operator is written as

$$\begin{aligned} P_s(t) &= \frac{1}{2} \{1 + s + \text{sgn}[\hat{\phi}'(t) - w] + \text{sgn}[-\hat{\phi}'(t) - w]\} \\ &= \theta(s[\hat{\phi}'(t) - w]) + \theta(-s[\hat{\phi}'(t) + w]) + \frac{1}{2}(s - 1). \end{aligned} \quad (55)$$

The dichotomic variable is defined so that we assign $Q = 1$ ($Q = -1$) when the absolute value of a result of a measurement of the coarse-grained field $\hat{\phi}'(t)$ is larger (smaller) than w . For the squeezed state defined by $|\psi_0\rangle = \prod_{k>0} S_k(\zeta_k)|0\rangle$, the expression of the quasiprobability distribution function is the same as Eq. (37) but with $A_{\text{sq}}(t)$, $B_{\text{sq}}(t_1, t_2)$, and $E(t)$ in this section. Figure 8 plots the contour of the quasiprobability distribution function $q_{1,1}(0, t_2)$ on the plane of wL

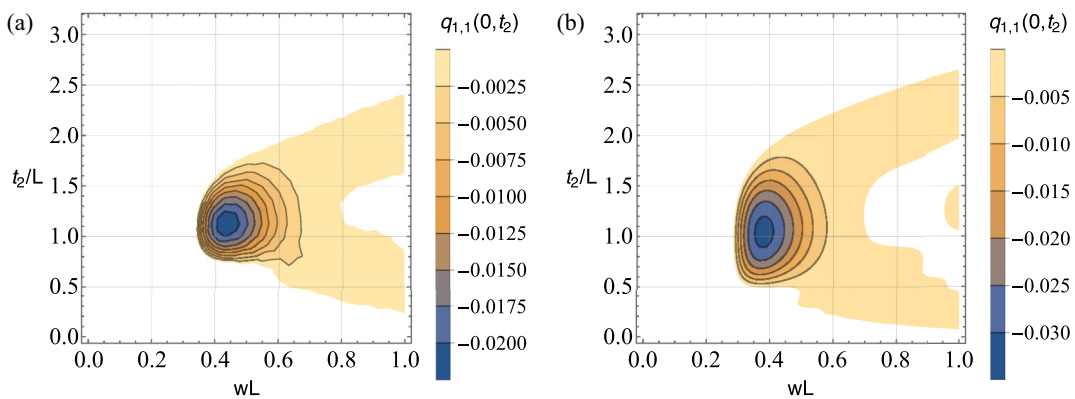


FIG. 8. Contour of $q_{1,1}(0, t_2)$ for the one-dimensional chiral massless field with the projection operator (55) on the plane of wL and t_2/L , where we fixed (a) $r = 0$ and (b) $r = 0.3$. In these panels, the quasiprobability takes negative values in the colored regions, where the Leggett-Garg inequality is violated.

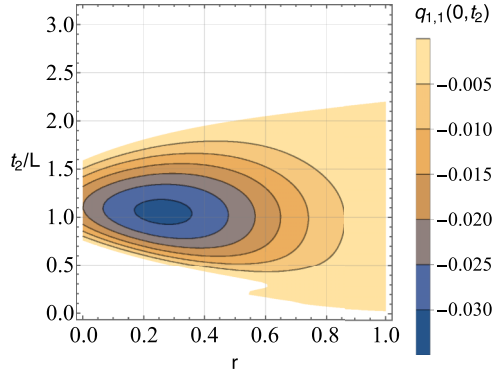


FIG. 9. Contour of $q_{1,1}(0, t_2)$ for the one-dimensional chiral massless field with the projection operator (55) on the plane of squeezed parameter r and t_2/L , where we fixed $wL = 0.4$.

and t_2/L for the vacuum state with $r = 0$ [Fig. 8(a)] and for the squeezed state with $r = 0.3$ [Fig. 8(b)]. We can see behaviors similar to the results of the three-dimensional model in Sec. II C (see Figs. 4 and 5). Similarly, Fig. 9 plots $q_{1,1}(0, t_2)$ on the plane of r and t_2/L . The quasiprobability distribution function has negative values smaller than -0.02 around $t_2/L \simeq 1.2$ and $wL \simeq 0.4 \sim 0.45$ even for the vacuum state. Figure 10 plots $q_{1,1}(0, t_2)$ as a function of t_2/L for the model with $wL = 0.45$ and $r = 0$ [Fig. 10(a)] and with $wL = 0.4$ and $r = 0.3$ [Fig. 10(b)]. For the vacuum state and the squeezed state, the expectation values of the coarse-grained value $\text{Tr}[\hat{\phi}'(t)\rho_0]$ is always zero. On the other hand, $q_{1,1}(0, t_2)$ is the quasiprobability that the measurement at $t_1 (=0)$ gives $|\hat{\phi}'(0)| > w$ and the measurement at t_2 gives $|\hat{\phi}'(t_2)| > w$. This is the counterintuitive result of measurements against the expectation values, which may occur due to a spread of the wave function and the superposition principle in quantum-mechanical systems.

IV. CONCLUSION

We have examined the violation of the Leggett-Garg inequalities for a quantum scalar field in a coherent state and the squeezed state with a coherent mode excitation, as well as the squeezed state and the vacuum state, where we constructed

the dichotomic variable of a coarse-grained field. We found that the violation of the Leggett-Garg inequalities may occur when $\xi \gtrsim 7$ and $1 \lesssim \ell L \lesssim 3.5$ for the (3 + 1)-dimensional quantum field in the one-mode coherent state. A similar violation appears for the (1 + 1)-dimensional chiral massless field, though the conditions for the violation are slightly different. We also demonstrated that the model of the one-mode coherent state with $\varphi(t) = 0$ is equivalent to the model of the vacuum state choosing $\varphi(t) = -E(t)$. Further, we demonstrated that a simple choice of the dichotomic variable and the projection operator exhibits violation of the Leggett-Garg inequalities for the vacuum state, as in Secs. II D and III C. Thus, by constructing the dichotomic variable properly, the violation of the Leggett-Garg inequalities can be observed for a quantum field in the vacuum state as well as the squeezed state. The violation of the Leggett-Garg inequalities occurs when the measurements give values opposite to the expectation values, which can be understood in analogy with a harmonic-oscillator model [22]. The periodic behavior in the quasiprobability distribution function, which appears in the case of a harmonic oscillator [22], does not appear for a coarse-grained quantum field. This could be understood as a kind of decoherence effect resulting from the fact that the dichotomic variable of the coarse-grained quantum field has a quantum correlation with the other region. Thus our finding demonstrates a possible use of the Leggett-Garg inequalities for testing the quantum nature of a field. We demonstrated the violations of the Leggett-Garg inequalities for the chiral massless quantum field in one dimension, which might be applied in an experiment of the quantum Hall system [28–30]. In the present work we did not consider any physical process of measurements of the dichotomic variable, which is constructed by a coarse-grained quantum field in a finite local region. Predictions connected to such a realistic experiment are left for future investigation (e.g., [31]).

ACKNOWLEDGMENTS

We thank Yasusada Nambu, Akira Matsumura, Tomoya Hirotsu, Youka Kaku, Yuki Osawa, Masahiro Hotta, Go Yusa, and Satoshi Iso for the discussions related to the topic in the present work. K.Y. was supported by JSPS KAKENHI (Grants No. JP22H05263 and No. JP23H01175). D.M. was supported by JSPS KAKENHI (Grant No. JP22J21267).

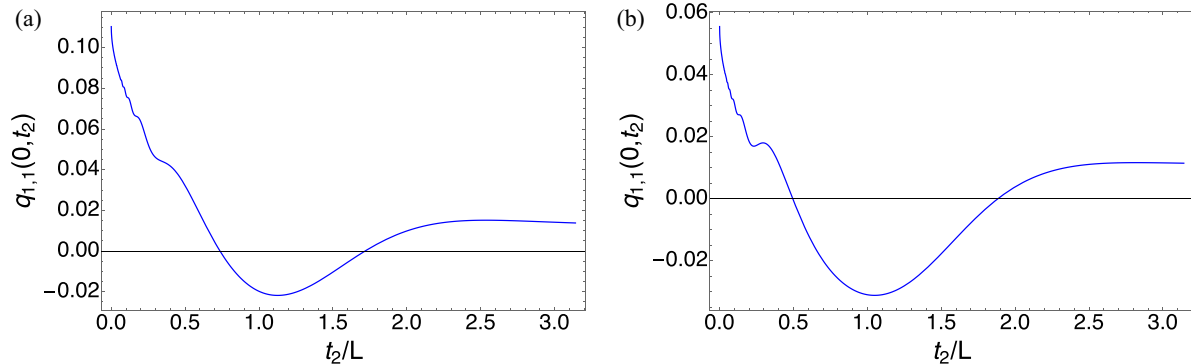


FIG. 10. Contour of $q_{1,1}(0, t_2)$ as a function of t_2/L for the one-dimensional chiral massless field in the vacuum state and squeezed state with the projection operator (55), where we fixed (a) $r = 0$ and $wL = 0.45$ and (b) $r = 0.3$ and $wL = 0.4$.

APPENDIX: USEFUL FORMULA FOR THE QUASIPROBABILITY DISTRIBUTION FUNCTION

Using the variables $c_1 = c \cos u$ and $c_2 = c \sin u$, the right-hand side of Eq. (30) leads to

$$\begin{aligned}
 q_{s_1, s_2}(t_1, t_2) = & \operatorname{Re} \left\{ \frac{1}{4\pi [A_{\text{sq}}(t_1)A_{\text{sq}}(t_2) - B_{\text{sq}}(t_1, t_2)]^{3/2}} \int_0^{\pi/2} du \exp \left(- \frac{A_{\text{sq}}(t_2)E(t_1)^2 + A_{\text{sq}}(t_1)E(t_2)^2 - 2B_{\text{sq}}(t_1, t_2)E(t_1)E(t_2)}{2[A_{\text{sq}}(t_1)A_{\text{sq}}(t_2) - B_{\text{sq}}(t_1, t_2)]^2} \right) \right. \\
 & \times \left[\frac{2[A_{\text{sq}}(t_1)A_{\text{sq}}(t_2) - B_{\text{sq}}(t_1, t_2)]^2}{A_{\text{sq}}(t_2)\cos^2 u + A_{\text{sq}}(t_1)\sin^2 u - s_1 s_2 \sin 2u} - \sqrt{2\pi} \left(\frac{A_{\text{sq}}(t_1)A_{\text{sq}}(t_2) - B_{\text{sq}}(t_1, t_2)^2}{A_{\text{sq}}(t_2)\cos^2 u + A_{\text{sq}}(t_1)\sin^2 u - s_1 s_2 B_{\text{sq}}(t_1, t_2) \sin 2u} \right)^{3/2} \right. \\
 & \times \exp \left(\frac{\{s_1 A_{\text{sq}}(t_2)E(t_1) \cos u + s_2 A_{\text{sq}}(t_1)E(t_2) \sin u - B_{\text{sq}}(t_1, t_2)[s_2 \sin u E(t_1) + s_1 \cos u E(t_2)]\}^2}{2[A_{\text{sq}}(t_1)A_{\text{sq}}(t_2) - B_{\text{sq}}(t_1, t_2)][A_{\text{sq}}(t_2)\cos^2 u + A_{\text{sq}}(t_1)\sin^2 u - s_1 s_2 \sin 2u B_{\text{sq}}(t_1, t_2)]} \right) \\
 & \times \operatorname{erfc} \left(\frac{s_1 A_{\text{sq}}(t_2)E(t_1) \cos u + s_2 A_{\text{sq}}(t_1)E(t_2) \sin u - B_{\text{sq}}(t_1, t_2)[s_2 \sin u E(t_1) + s_1 \cos u E(t_2)]}{2[A_{\text{sq}}(t_1)A_{\text{sq}}(t_2) - B_{\text{sq}}(t_1, t_2)]} \right) \\
 & \times \sqrt{\frac{2[A_{\text{sq}}(t_1)A_{\text{sq}}(t_2) - B_{\text{sq}}(t_1, t_2)^2]}{A_{\text{sq}}(t_2)\cos^2 u + A_{\text{sq}}(t_2)\sin^2 u - 2s_1 s_2 B_{\text{sq}}(t_1, t_2) \sin 2u}} \\
 & \left. \times \{s_1 A_{\text{sq}}(t_2)E(t_1) \cos u + s_2 A_{\text{sq}}(t_1)E(t_2) \sin u - B_{\text{sq}}(t_1, t_2)[s_2 E(t_1) \sin u + s_1 E(t_2) \cos u]\} \right\},
 \end{aligned}$$

where $\operatorname{erfc}(z)$ is the complementary error function.

-
- [1] A. J. Leggett and A. Garg, *Phys. Rev. Lett.* **54**, 857 (1985).
 - [2] A. J. Leggett, *J. Phys.: Condens. Matter* **14**, R415 (2002).
 - [3] C. Emary, N. Lambert, and F. Nori, *Rep. Prog. Phys.* **77**, 016001 (2014).
 - [4] J. F. Clauser, M. A. Horne, A. Shimony, and R. A. Holt, *Phys. Rev. Lett.* **23**, 880 (1969).
 - [5] R. Ruskov, A. N. Korotkov, and A. Mizel, *Phys. Rev. Lett.* **96**, 200404 (2006).
 - [6] A. Palacios-Laloy, F. Mallet, F. Nguyen, P. Bertet, D. Vion, D. Esteve, and A. N. Korotkov, *Nat. Phys.* **6**, 442 (2010).
 - [7] J.-S. Xu, C.-F. Li, X.-B. Zou, and G.-C. Guo, *Sci. Rep.* **1**, 101 (2011).
 - [8] J. Dressel, C. J. Broadbent, J. C. Howell, and A. N. Jordan, *Phys. Rev. Lett.* **106**, 040402 (2011).
 - [9] G. C. Knee, K. Kakuyanagi, M.-C. Yeh, Y. Matsuzaki, H. Toida, H. Yamaguchi, S. Saito, A. J. Leggett, and W. J. Munro, *Nat. Commun.* **7**, 13253 (2016).
 - [10] E. Kreuzgruber, R. Wagner, N. Geerits, H. Lemmel, and S. Sponar, [arXiv:2307.04409](https://arxiv.org/abs/2307.04409).
 - [11] X.-Z. Wang and B.-Q. Ma, *Eur. Phys. J. C* **82**, 133 (2022).
 - [12] A. Santini and V. Vitale, *Phys. Rev. A* **105**, 032610 (2022).
 - [13] A. Matsumura, Y. Nambu, and K. Yamamoto, *Phys. Rev. A* **106**, 012214 (2022).
 - [14] S. V. Moreira, A. Keller, T. Coudreau, and P. Milman, *Phys. Rev. A* **92**, 062132 (2015).
 - [15] S.-S. Majidy, H. Katiyar, G. Anikeeva, J. Halliwell, and R. Laflamme, *Phys. Rev. A* **100**, 042325 (2019).
 - [16] S. Majidy, J. J. Halliwell, and R. Laflamme, *Phys. Rev. A* **103**, 062212 (2021).
 - [17] S. Goldstein and D. N. Page, *Phys. Rev. Lett.* **74**, 3715 (1995).
 - [18] J. J. Halliwell, *Phys. Rev. A* **93**, 022123 (2016).
 - [19] J. J. Halliwell, *Phys. Rev. A* **96**, 012121 (2017).
 - [20] J. J. Halliwell, H. Beck, B. K. B. Lee, and S. O'Brien, *Phys. Rev. A* **99**, 012124 (2019).
 - [21] J. J. Halliwell, A. Bhatnagar, E. Ireland, H. Nadeem, and V. Wimalaweera, *Phys. Rev. A* **103**, 032218 (2021).
 - [22] K. Hatakeyama, D. Miki, M. Tani, Y. Yamasaki, S. Iso, A. S. Adam, A. Rohim, and K. Yamamoto, [arXiv:2310.16471](https://arxiv.org/abs/2310.16471).
 - [23] S. Bose, D. Home, and S. Mal, *Phys. Rev. Lett.* **120**, 210402 (2018).
 - [24] C. Mawby and J. J. Halliwell, *Phys. Rev. A* **105**, 022221 (2022).
 - [25] C. Mawby and J. J. Halliwell, *Phys. Rev. A* **107**, 032216 (2023).
 - [26] D. Das, D. Home, H. Ulbricht, and S. Bose, *Phys. Rev. Lett.* **132**, 030202 (2024).
 - [27] A. Asadian, C. Brukner, and P. Rabl, *Phys. Rev. Lett.* **112**, 190402 (2014).
 - [28] M. Hotta, Y. Nambu, Y. Sugiyama, K. Yamamoto, and G. Yusa, *Phys. Rev. D* **105**, 105009 (2022).
 - [29] G. Yusa, W. Izumida, and M. Hotta, *Phys. Rev. A* **84**, 032336 (2011).
 - [30] Y. Nambu and M. Hotta, *Phys. Rev. D* **107**, 085002 (2023).
 - [31] T. Hirotoni, Y. Nambu, A. Matsumura, and K. Yamamoto, [arXiv:2401.10692v1](https://arxiv.org/abs/2401.10692v1).